2012

Gorham's Cave sediment micromorphology

Paul Goldberg
Boston University, goldberg@uow.edu.au

Richard I. M Macphail
University College London

Publication Details

Goldberg, P. & Macphail, R. I. (2012). Gorham's Cave sediment micromorphology. In R. N. E. Barton, C. B. Stringer & J. C. Finlayson (Eds.), Neanderthals in Context: a report of the 1995-1998 excavations at Gorham's and Vanguard Caves, Gibraltar (pp. 50-61). Oxford, United Kingdom: Oxford University School of Archaeology.

Gorham's Cave sediment micromorphology

Abstract
[extract] Introduction Fieldwork, sampling and sediment micromorphology together with X-Ray EDAX and bulk sample analyses were carried out at Gorham's Cave.

Disciplines
Medicine and Health Sciences | Social and Behavioral Sciences

Publication Details
Goldberg, P. & Macphail, R. I. (2012). Gorham's Cave sediment micromorphology. In R. N. E. Barton, C. B. Stringer & J. C. Finlayson (Eds.), Neanderthals in Context: a report of the 1995-1998 excavations at Gorham's and Vanguard Caves, Gibraltar (pp. 50-61). Oxford, United Kingdom: Oxford University School of Archaeology.

4 Gorham's Cave sediment micromorphology

P. Goldberg and R. I. Macphail

Introduction

Fieldwork, sampling and sediment micromorphology together with X-Ray EDAX and bulk sample analyses were carried out at Gorham's Cave. The site's micromorphology was first studied by Goldberg in 1989 and was followed by further work at Gorham's Cave (1995, 1996, 1998), as well as new studies at Vanguard Cave during the same latter period; results are reported in Goldberg and Macphail (2000), and Macphail and Goldberg (2000). To achieve consistency within the present volume this current presentation attempts to follow the lithostratigraphic units identified in Chapter 2. It should be noted, however, that stratigraphic sections exposed in 1989 and later are not necessarily those observed at the end of the 1990s, because of erosional events, slumping and excavation. In Appendix 4.1, 'sediment types' have been simply termed Guano, Hearth, Sand and Silt; in the text below, bulk analyses refer to these broad categories for different lithostratigraphic units. Micromorphological analysis also revealed broad microfacies characteristics, including B (burrows), Ca (calcium carbonate), G (guano), Om (organic matter), S (sand) and Si (silt); details of these microfabrics are described according to lithostratigraphic unit/sample (see Chapter 13).

As is apparent from the profiles and descriptions below, the cave does not present a simple vertical stratigraphic section (Chapter 2). For example, the stratigraphically highest sediments are exposed further back in the cave, where conditions are quite damp (dripping water, reduced evaporation, greater abundance of bats, etc.), and where diagenesis (e.g. calcification, decalcification, leaching and phosphatization) is more likely to be common. In contrast, the stratigraphically oldest deposits are situated nearer the front of the cave, which is more exposed, effectively drier, and closer to the source of sand exterior to the cave. We also note micromorphological evidence that substantiates field observations that the roof of the cave mouth has receded, i.e., the current morphology of the cave mouth does not reflect the original extent of the cave seawards. Thus, the geological history of the site (depositional and both syn- and post-depositional events) is pieced together from these stepped exposures.

Fieldwork was complemented by a micromorphological study of 95 thin sections and the analysis (organic matter by loss on ignition – LOI at 550°C, magnetic susceptibility, phosphate (as total P) and pH) of 50 associated bulk samples (Goldberg and Macphail 2000; Macphail and Goldberg 2000). We present here only a selection of all the collected thin sections, but for archival purposes all thin section samples are indicated in Figure 4.1. Methods are described in Chapter 13; the 1989 thin sections were analysed semi-quantitatively. The location of thin section samples is indicated in Figure 4.1, and bulk samples and data are listed in Appendix 4.1. Multiple samples and coprolites (see Chapter 19) were prepared for pollen analysis, but all were found to be devoid of pollen (Gill Cruise, pers. comm.). It is important to note that because the sediment micromorphology at Gorham's Cave was carried out in parallel with studies of the simpler sequence at Vanguard Cave (Chapter 13), we often refer to processes that were clearly observed and investigated at this second site, including the use of microprobe for example.

Results

Results are presented unit by unit (see Fig. 4.1; Chapter 2).

Cemented Hearths (CHm.1–5)

Thin section sample Gor96-52 records an ash-rich hearth that was highly organic (8.1% LOI) and yielded the highest magnetic susceptibility values (χ=418 × 10^{-8} SI/Kg) recorded at Gorham's Cave (Appendix 4.1).

Overall, these deposits are characterized by being organic rich in places, and locally, layers contain numerous hyaena coprolites (e.g. samples Gor89-23, Gor96-51) that indicate extensive denning of hyaenas (thus suggesting periodic abandonment of the site by humans, as both do not normally occupy the same space at the same time). Furthermore, many of these deposits (e.g. Gor96-51) are indurated with microsparite, typically with radiating crystals (meniscus cement), which were likely tied to conditions of inundation associated with dripping water, and indicative of a wetter period, particularly in the upper part. Interestingly, some samples (e.g. Gor89-21) show that this cementation pre-dates a diagenetic phosphatization phase where apatitic crusts can be seen to replace some of this calcite (Figs. 4.2 and 4.3). This sequence – of unknown length – took place relatively rapidly on the former surface, although its total duration cannot be determined.

In addition, both intact and partly disturbed combustion features were seen. In sample Gor96-53, for example (Figs. 4.4 and 4.5), we observed a chaotic mixture of burned bone, charcoal and rounded soil/silty clay aggregates, which would point to a trampled combustion feature or one that has been reworked by cleaning (e.g. rake-out and see Fig. 4.24). The lack of calcareous ashes associated with this sample is due to either incomplete combustion (note the abundance of charcoal) and/or dissolution of carbonate (which is not shown in the micrograph but can be observed in the upper part of the slide, in which only patchy remains

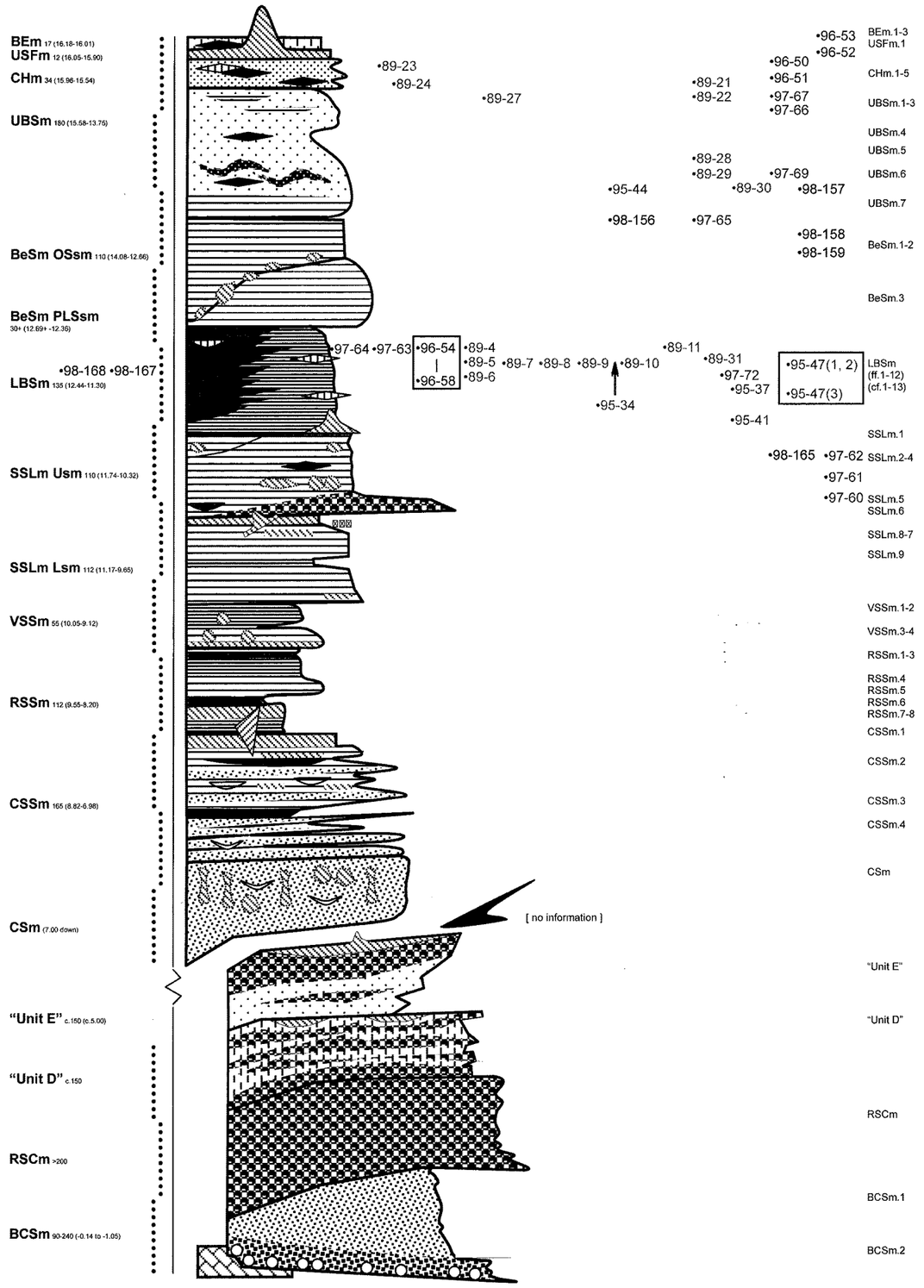

Fig. 4.1 Gorham's Cave, micromorphology sample locations in relation to lithostratigraphic units (see Chapter 2).

Fig. 4.2 Micromorphology thin-section sample Gor89/21; detail showing square piece of travertine in the lower right-hand corner and charcoal in the centre. The upper surface of the travertine has been phosphatized, a common phenomenon in these uppermost samples in the cave. PPL (plane-polarized light), frame width is ~3.9 mm. Photo: P. Goldberg and R. Macphail. (Colour versions of all thin sections available online.)

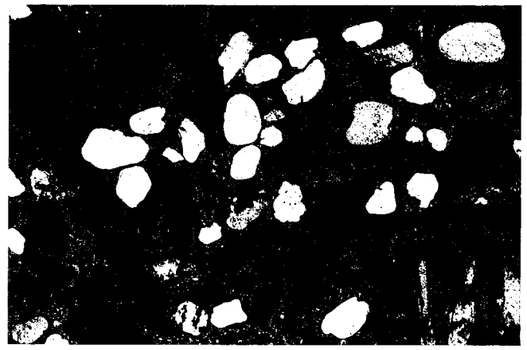

Fig. 4.3 Micromorphology thin-section sample Gor89/21 in XPL (crossed-polarized light); note that the calcite in the vughs (particularly in centre) is made of subsequent crystals of calcite meniscus cements, which are likely to result from saturation of dripping water rather than inundation with groundwater (Scholle and Ulmer-Scholle, AAPG Memoir 77). These cements are typical in these uppermost deposits. Photo: R. Macphail and P. Goldberg.

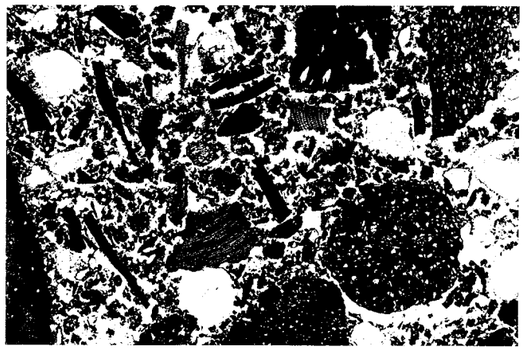

Fig. 4.4 Micromorphology thin-section sample Gor96/52; burned bone and charcoal mixed with quartz and fluffy silty clay associated with biological reworking by small fauna associated with guano; evidence of locally reworked combustion feature. PPL, frame width is ~3.9 mm. Photo: P. Goldberg and R. Macphail.

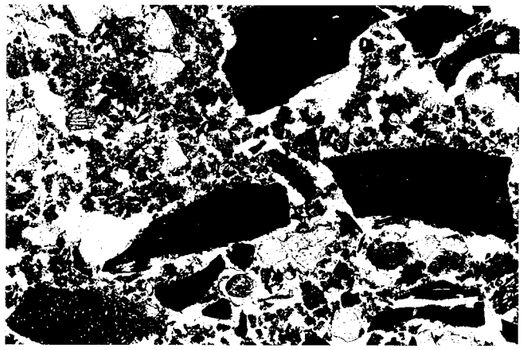

Fig. 4.5 Micromorphology thin-section sample Gor96/52; similar to Fig. 4.4, with chaotic mixture of burned bone, charcoal and rounded soil/silty clay aggregate. This appears to represent a trampled combustion feature or one that has been reworked by cleaning (e.g. rake-out). The lack of calcareous ashes associated with this sample is due to either incomplete combustion (note the abundance of charcoal) and/or dissolution of carbonate (which is not shown here but can be observed in the upper part of the slide, in which only patch remains of calcite are preserved). PPL, frame width is ~3.9 mm. Photo: P. Goldberg and R. Macphail.

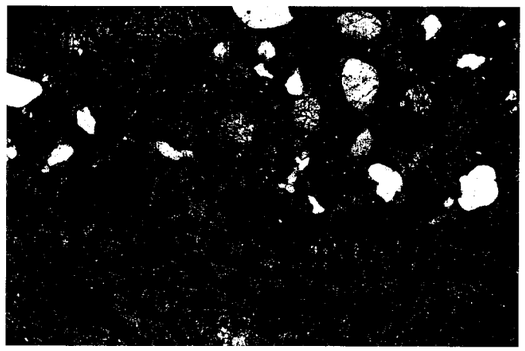

Fig. 4.6 Micromorphology thin-section sample Gor97/67; ash-cemented bone; bone fragment at the base filled with sparry calcite, perhaps representing recrystallized calcareous ashes. The overlying matrix is phosphatic clay. XPL, frame width is ~3.9 mm. Photo: P. Goldberg and R. Macphail.

of calcite are preserved). In sample Gor97-67 (Fig. 4.6), a bone fragment at the base of the thin section is infilled with sparry calcite, which may be the remains of recrystallized calcareous ashes. This cementation likely pre-dates sealing-in of this bone by phosphate-rich clay.

Finally, we note in sample Gor96-53 that numerous sand-size grains are coated with organic silty clay, which we interpret to indicate rolling of material downslope; the massive, unbedded nature of the sand in this sample would support this interpretation.

Upper Bioturbated Sands (UBSm.1–7)

UBSm deposits comprise interbedded sand and organic silty sand, rich in coprolites, phosphatized limestone clasts, small bones and soil animal excrements representing reworking of guano, as well as ash residues (see samples

Fig. 4.7 Macroscan of thin-section of Gor97/69c from monolith thin-section sample series Gor97/69a, 69b, 69c, showing interbedded sand and phosphate-rich layers (see Fig. 4.8). Frame width is ~50 mm. Photo: P. Goldberg and R. Macphail.

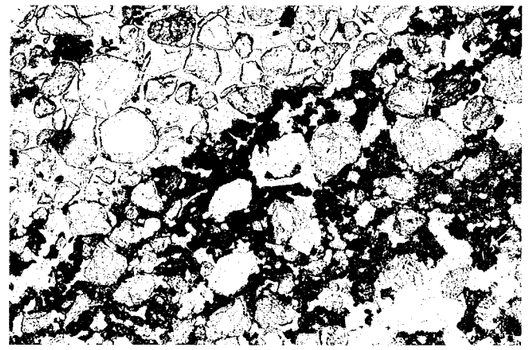

Fig. 4.8 Micromorphology thin-section sample Gor97/69c; typical bedded phosphatic surface crust within overall sandy phosphate mix (see Fig. 4.7). Note the sharp contact between the crust and the loose sand above, indicating at least a short period of exposure during which the guano-derived crust formed. PPL, frame width is ~3.9 mm. Photo: P. Goldberg and R. Macphail.

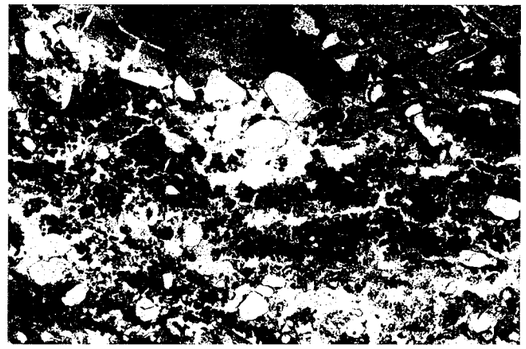

Fig. 4.9 Micromorphology thin-section sample Gor89/28b; finely bedded organic matter and silty organic clay. Note the fine pellety nature of some of the reddish material, microfaunal excrements. At the upper part is a partially phosphatized piece of bedrock; phosphate is in the form of apatite. PPL, frame width is ~3.9 mm. Photo: P. Goldberg and R. Macphail.

Gor97-69a, Gor97-69b and Gor97-69c; Fig. 4.7). The macro views of these samples clearly show continuous and discontinuous phosphate-rich layers (e.g. sample Gor97-69c contains a well developed silty phosphatic layer within the overall sandy deposit; Fig. 4.8) or clumps of phosphate worked into the sandy matrix by biological reworking as shown by the porous nature of the lower half of the sample. In sample Gor89-29 from Square C98, sand is intercalated with organic silty clay of variable thickness that contains phosphatic crusts and hyaena coprolites, along with some bone. In the overlying sample Gor89-28, limestone clasts show apatitic weathering rinds, which rest upon sand and finely laminated charcoal and phosphatic silty clay (Fig. 4.9). Some of this fine fraction exhibits a flecked/pellety nature indicative of microfaunal reworking of guano material (Shahack-Gross *et al.* 2004).

Eight bulk samples from UBSm were analysed (Appendix 4.1). Typically, sandy microfacies are very poorly organic (0.1–0.6% LOI), with low amounts of phosphorus (810 ppm P) as compared to hearths (2.5–5.0% LOI; e.g. 41,800 ppm P) and guano layers (0.5–4.1% LOI; 1890–32,800 ppm P). Some silty layers are also humic (5.9% LOI) and evidently contain burned mineral material (χ=167 × 10^{-8} SI/Kg) presumably eroded from hearths. It can also be noted that whilst minerogenic sands are highly alkaline (pH 9.1), silts containing organic matter are less so (pH 7.8).

Bedded Sands (BeSm) and Orange Sand (BeSm(OSsm).1–2)

The erosional nature of the sand is shown in thin section Gor97-65e that comes from the very top of the BeSm, which directly underlies the UBSm. The fact that the relatively clean sand erodes phosphatic, dusty silty sand and shows a vertical and sharp contact demonstrates that the underlying material must have been compacted. In addition, it demonstrates that for this material to be eroded, there must have been a certain existing topographic relief to permit this erosion: i.e. a flat surface would not result in erosion. This latter point also supports the notion that the inclinations and wavy nature of the overlying UBSm are not solely due to soft sediment deformation but also

Fig. 4.10 Gorham's Cave during 1997 season showing faulting and slumping of lower part of UBSm; these deposits have a 'downthrown' side on the right (north).

result from a certain degree of subsidence of the underlying substrate (Fig. 4.10).

Lower Bioturbated Sands Fine Facies (LBSmff.1–12)

LBSmff was sampled extensively in Square C99 in the form of two overlapping core/monoliths (Gor95-47 Cores 1–2 represent an interval apparently near the top of the LBSmff, approximately LBSmff.1; Gor95-47 Core 3 likely falls within the sequence LBSmff.2–4). In addition, 17 associated bulk samples were analysed (e.g. as subsampled from monoliths Gor97-63, Gor97-64 and Gor97-72).

Gor95-47 is composed of finely bedded to laminated, organic matter-rich clays and sands that tend to thicken towards the centre of the cave. The bottom third or so is characterized by two thick ashy sand lenses that appear truncated at the top. In 1997 additional samples were studied. These include two samples:

Sample Gor97-63. The lower ~50 cm or so of the monolith is generally sandier, more massive, and lighter in colour than the upper part which seems to contain an ashy lens and associated burned substrate. Above, at ~12 m, there is a shift to more of an organic facies grading up to finely laminated waterlain sediments. Gor97-64 is the lateral equivalent to 97-63 and consists of finely laminated organic clays and silts and coarse bedded brown sands. Brown laminae are more compact than the silty and sandy ones. Basically three subunits were observed:

a dark reddish brown (5YR3/3), massive to crudely bedded, organic-rich sand with flecks of red (fire-reddened clay);
b dark red (2.5YR5/4) organic clay, finely laminated;
c strong brown (7.5YR5/4), laminated to coarsely bedded, organic-rich sand, which is not apparently phosphatized but appears to be burrowed.

Sample Gor97-72 is a large block forming an upward continuation of 97-63 and comprises finely laminated, organic-rich silty/sandy clay. Basically two subunits occur: a) 5YR3/2 dark red brown with some pale brown spots that in hand lens appear to represent washed sands devoid of matrix; very fluorescent in UV indicative of phosphatic organic matter; and b) similarly 5YR3/2 dark reddish brown but with lower fluorescence under UV, and is darker brown and or red at the very bottom of this subunit.

Lower Bioturbated Sands Coarse Facies (LBSmcf.1–13)

Micromorphological data support the field observations (Chapter 2), with the sediments being quite sandy. Yet, different types of inclusions were observed:

- eggshell and a phosphatic dropping (e.g. sample Gor96-55);
- charcoal, bone, shell and bands of organic silty clay (e.g. sample Gor96-56);
- interbedded, organic silty clay and sand (e.g. samples Gor95-39, Gor96-41b, Gor96-41c).

It appears that much of this material is waterlain (cf. bedding in sample Gor89-21 from CHm.2), although it differs from the 95-47 series of LBSmff, which is much finer, and is situated closer to the central axis of the cave where one might expect to have pooling/ponding of water.

Bulk data reflect the mixed microfacies characteristics of the sediment types (Appendix 4.1), with sands (mean 1.15% LOI, n=6; 5060–17,800 ppm P) showing the inclusion of phosphatic grains, although less organic- and phosphate-rich compared to guano-rich layers (mean 4.0% LOI, n=8; mean 24,460 ppm P, n=8, range 9160–72,100 ppm P). EDAX analysis of guano in sample 89-9b clearly showed peaks of Ca and P (presumed hydroxyapatite or dahllite; cf. Wattez *et al.* 1990) (Fig. 4.21). Hearths/combustion zones also show enrichment in organic matter and phosphorus (2.6–6.3% LOI; 7860–31,000 ppm P).

Sands & Stony Lenses (SSLm(Usm))

In sample Gor97-62 from Square D105, for example, the sand appears generally as a micrite-cemented blown sand, with many coarse bone fragments (see bulk analyses below), and some limestone. Most of the sand fraction is coated with a clotted clayey micrite, and we see more than one phase of post-depositional cementation: the first clotted micrite phase is followed by microsparite filling in the remaining void space. Rounded bone fragments suggest movement/rolling and possible sandblasting. Furthermore, the vertical orientation of the bone suggests some reworking (e.g. trampling or bioturbation) when the sand was still unconsolidated and mobile.

Further out towards the entrance in Square B108 in SSLm(Usm).2 (e.g. sample Gor98-165), we observe essentially a massive to finely bedded sandy deposit with thin stringers and zones of phosphatic guano crusts (as clumps and remnants of stabilized surfaces); some charcoal and burned bone

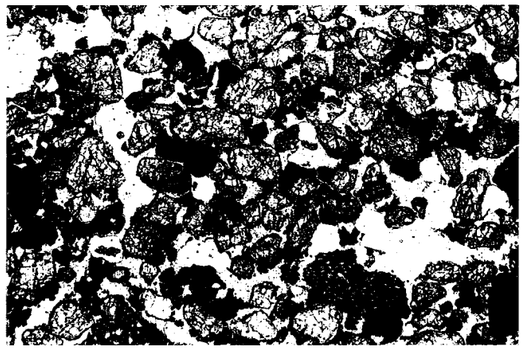

Fig. 4.11 Gor98/165; sands containing guano; phosphatic crust on burned bone. Overall these sediments show moderate phosphate enrichment (see Fig. 4.1). PPL, frame width is ~3.9 mm. Photo: P. Goldberg and R. Macphail.

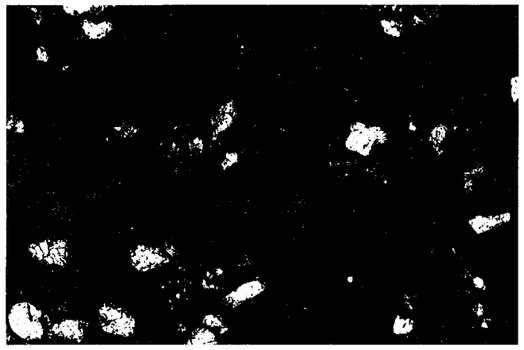

Fig. 4.12 Micromorphology thin-section sample Gor98/165; sands containing guano; phosphatic crust on charred or humified organic matter. XPL, frame width is ~3.9 mm. Photo: P. Goldberg and R. Macphail.

(reworked from hearths?) are preserved, and in some cases are covered with a phosphatic crust (Figs. 4.11 and 4.12).

Bulk analyses show, once again, that sands are generally poorly humic (0.2–1.4% LOI), but included bone and guano have led to moderate enrichment in phosphorus (1700–2630 [97-62] ppm P).

Lower units

For the following units it has not been possible to provide an absolute correlation with the new lithostratigraphic sequence for the cave. We have therefore reverted to our original descriptions and each of the micromorphological samples is described according to depth and position in the cave. Two similar-looking samples are described from near the top of the lower units, Gor98-154 and Gor98-155, that are rather alike both in the field and in thin section. In the field they appear as finely bedded to laminated, dark reddish brown organic silty clay sand with charcoal fragments and white limestone clasts. In thin section (both Gor98-154a and Gor98-154b), we observe finely bedded sand interbedded with organic-rich clay. Scattered throughout the sample are fragments of bone and coprolites of both carnivore (see Figs. 4.22 and 4.23) and bird guano origin; some of the bone is burned and also exhibits calcareous ash adhering to it. Localized domains of ash that are irregularly incorporated into the matrix attest to the reworking of ash along with slaking crusts composed of bedded silt and organic-rich clay. Moreover, we see that this type of deposition and reworking of sand and silty/clayey slaking crusts by run-off has resulted in the incorporation of bone fragments – some of which are burned – and calcareous ash. It points to previously existent combustion features that were in cases penecontemporaneously reworked in antiquity and redeposited. Biological inputs of carnivore coprolites and phosphatic bird guano indicate the presence of former exposed surfaces.

Sample Gor98-155 is similar at the base but the overlying part is more sandy and cleaner. Hyaena coprolites, shell fragments and charcoal pieces have been reworked by water.

Many samples were collected from reddish sands of the lower units in the entrance of the cave, in and near Square G111 (samples Gor89-12 through to Gor89-17). These samples are overall similar in make-up but different in proportions and arrangements of the sand and finer fractions. Sample Gor89-12, for example, is close to the top of this sampled sequence and comprises quartz sand, charcoal, coprolite fragments, bone (some of which is rounded), and bright reddish yellow phosphatic chunks of guano crusts; the fine fraction is in the form of coarse sand/granular aggregates that are organized into diffuse, non-continuous laminae, and locally the clay contains silt-size inclusions of brown, fibrous organic matter. Fragments of guano crusts and guano occur as orange brown isotropic inclusions that are highly autofluorescent under blue light epifluorescence (Figs. 4.13 and 4.14). The fine fractions represent interstitial, mesofauna-worked (pellets) guano-rich cave earth. In addition, the deposit exhibits rip-up clasts reworked from nearby sediments by sheet flow and mud flow.

Similar types of sediments, although with a higher proportion of fine material, are seen in sample Gor89-13. Here, the coarse fraction in this sample is composed mostly of quartz sand, which takes the form of distinct laminae or is porphyrically distributed throughout the finer fraction of the sample. In addition, sand- and granule-size coprolite grains are fairly abundant (*c.*3 per cent). Localized graded bedding of coarse to fine silt, especially rich in mica, implies some sheet flow. Some bone fragments were observed, as well as phytoliths. Other coarse components in this sample are a sand-size, red brown clay papule, and a rounded, sand-size herbivore faecal pellet. One fragment of phosphatized limestone was observed.

The red brown, organic-rich fine fraction exhibits paler yellow brown mm-size domains; these areas have a tendency to be isotropic and are probably phosphatic. The latter are supported by their high degree of autofluorescence under blue light illumination. In addition, the matrix locally contains silt-size inclusions of detrital calcite, in the form of either mosaic sparite or micritic aggregates; these are also present in graded beds. At higher magnifications (e.g. 200×), the matrix is seen to be composed of finely comminuted, reddish brown organic debris, which is also autofluorescent and appears to be guano.

Sample Gor89-14 is similar and photomicrographs in blue light epifluorescence show the phosphatic nature of individual grains that make up an otherwise homogeneous

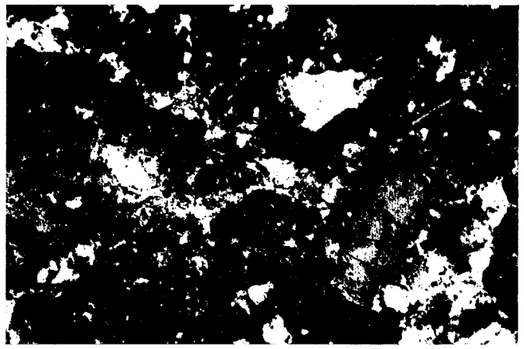

Fig. 4.13 Micromorphology thin-section sample Gor89/14; detail of undifferentiated mass of reddish brown and speckled orange brown fragments with an angular quartz grain at the top. PPL, frame width is ~1.2 mm. Photo: P. Goldberg and R. Macphail.

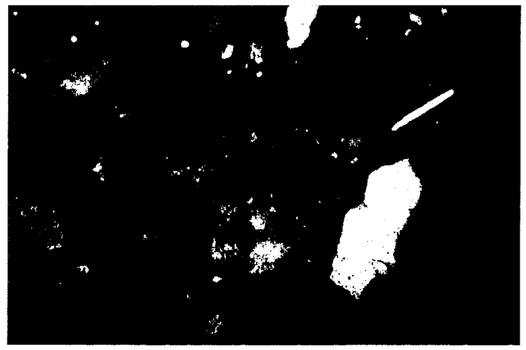

Fig. 4.14 Micromorphology thin-section sample Gor89/14, as at left, but under blue light epifluorescence. The bright grains are apatite derived from guano that have been incorporated into the organic clayey matrix. Blue light (BL), frame width is ~1.2 mm. Photo: R. Macphail and P. Goldberg.

and undifferentiated yellow brown fine fabric in visible light (see Figs. 4.13 and 4.14).

Sample Gor89-17 is noteworthy by the inclusion of large amounts of weathered calcareous ash aggregates and bone which is dusted with ash, a fragment of burned eggshell, and roof fall. The lack of structure of these burned components, such as we would witness in an *in situ* combustion feature, indicates reworking of hearths and implies occupation upslope from this location.

In all, these samples represent organic-rich guano deposits mixed with sand and inputs of finer silty clays derived from undifferentiated mud flows and layered sheet flows. These flows have resulted in the reworking of many of these components from perhaps *in situ* locations and combustion features, resulting in redistribution of ashes and bones. These deposits have been accompanied by inputs of phosphate-rich guano producing phosphatic surface crusts on stabilized and exposed surfaces.

Nine bulk samples were analysed, including guano, silts and sands, and these recorded an enhanced magnetic susceptibility (mean $\chi=200 \times 10^{-8}$ SI/Kg, $n=4$; range $\chi=100\text{-}302 \times 10^{-8}$ SI/Kg; Appendix 4.1). These values clearly corroborate the identification of hearth debris in thin section. Guano layers (mean 6150 ppm P, range 990–10300 ppm P, $n=3$) generally show far less magnetic susceptibility enhancement that is indicative of included burned materials (mean $\chi=71 \times 10^{-8}$ SI/Kg; range $\chi=24\text{-}230 \times 10^{-8}$ SI/Kg; $n=5$).

Three samples were observed below those of the reddish sands (samples 89-12 through 89-17). These samples (Gor89-18, Gor89-20 and Gor89-19, from top to bottom) are not dissimilar to the overlying ones in terms of basic composition, but there are some clear differences. Sample Gor89-18, for example, macroscopically shows bedding, with a *c.*2 cm band of more cemented sand running through the middle of the sample. Overall, in comparison to the clayey ones above, this sample appears somewhat less biological and more 'chemical' in character, with extensive calcite precipitation. There are abundant mm-size, well rounded quartz (~20 per cent) but relatively few bones coprolites and charcoal. Coprolites are in fact virtually absent, and bone (~1 per cent) often displays rounded edges, possibly due to digestion or other chemical attack. A few isolated echinoderm fragments occur, with some shell fragments (2 per cent) and cemented bioclasts; the last are probably derived from aeolianite deposits found just above the cave. In addition, fragments of travertine are less abundant than in sample Gor89-17 and are smaller in size; some tufa grains ~1 mm in diameter were observed.

The matrix is composed of calcareous clay with micritic coatings that range in thickness from ~60 to 200 μm. Many of these coatings, as well as the 'travertine fragments', look algal, particularly in the lower part of the slide where aggregates and domains of the original red clay have been invaded by micritic calcite. These commonly take on a rounded clotted morphology ~100 μm in diameter, but it is not clear whether this reflects an original depositional feature or one due to break up of original fabric by calcite impregnation. Some of the clayey and calcareous grains are clearly polygenetic, showing several phases of formation. It seems that the micritic impregnation of most of the groundmass is responsible for the pink colour observed in the field. Finally, we note the presence of eggshell, perhaps as a non-cultural accumulation from nests in the walls and ceiling; bone is embedded in micrite, which is in part derived from ash. In sum, we interpret this sample as representing calcareous mud flows, dipping towards the rear of the cave, which transported many kinds of materials, including limestone, shell and sands, as well as guano reworked mesofauna pellets and ash aggregates that are cemented on to the bone. Eventually the deposits were partially re-cemented in their present position.

A cemented lens in this deposit (sample Gor89-20; see field photo showing light- coloured wedge which thickens to the right – north) was observed in the field and became more indurated towards the north. In thin section, most of the sample is clay-free and generally consists of rounded coarse sand and granules comprising principally siliceous grains (quartz, quartzite), clayey aggregates, and tufa-like fragments and bioclasts, which tend to be more abundant and coarser at the bottom. Cementation is patchy. Where it is massive, it consists of fine micritic envelopes (~10 μm thick) around grains superposed by microsparite that occludes the pores (Figs. 4.15 and 4.16). Such massive cementation occurs only locally. At the base, remnants of

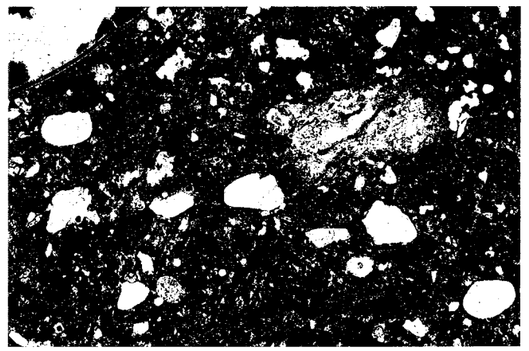

Fig. 4.15 Micromorphology thin-section sample Gor89/20; reddish brown domains of organic-rich clay and quartz sand cemented by microsparite; in the centre right is a yellow, irregularly shaped, phosphatized piece of guano. PPL, frame width is ~3.9 mm. Photo: P. Goldberg and R. Macphail.

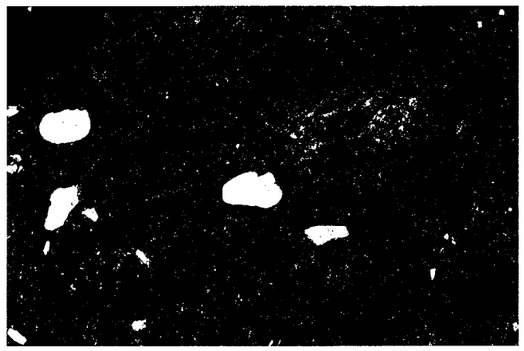

Fig. 4.16 Micromorphology thin-section sample Gor89/20 in XPL; note the porosity within the fine calcite and the isotropic nature of the guano fragment described above. Photo: P. Goldberg and R. Macphail.

the underlying unit can be found; these consist of micritic impregnations of more poorly sorted clayier material containing clayey aggregates as in sample Gor89-19. Elsewhere, grains show patchy rims and braces of micrite, ~10 to 20 μm thick.

The sequence of events for Gor89-20 thus appear to be:

1 sand deposition;
2 micritic coatings and fine fabric;
3 localized amorphous organic mesofauna pellets; and finally,
4 microsparitic partial cementation (Figs. 4.15 and 4.16).

The last event represents meteoric phreatic conditions associated with the flowstone crust. The pelletal fabrics show influence of guano. Whilst this sample is notably rich in rounded marine bioclasts (e.g. sea urchin spines among others), their absence in other samples could be related to decalcification of the deposits. Thus, while a marine origin is tempting, it is not unequivocal, especially in light of the presence of clasts of cave roof and tufa, which point to a location within the cave receiving subaerial gravity-derived clasts.

Eleven bulk samples were analyzed and clearly show variations in sediment composition. Sands (mean 1.5% LOI, range 0.1–4.0% LOI, $n=6$; mean 2510 ppm P, range 410–2660 ppm P, $n=8$) clearly show a marked variation in amounts of included organic matter and phosphate materials, as noted in thin section. An example of the silts (1.0% LOI; 1970 ppm P) clearly contrasts with guano-rich layers (4.3–4.5% LOI; 7270–14,700 ppm P).

Exposed in Square H113 is a sequence of sandy deposits with alternately bedded whitish and reddish bands. Sample Gor89-01 comes from a lighter band in the sequence and comprises rounded to subround quartz grains and rock fragments (including travertine fragments) with relatively little matrix. The latter consists of small (75 μm) clayey aggregates within intergranular pores or as discontinuous patches or coats around quartz grains. A few grains of limpid bright yellow and reddish amber clay papules occur. It is locally cemented with micrite (in some cases clayey micrite), some in the form of nodules; however, most calcite appears to be undergoing dissolution. Sample Gor89-3 is from a slightly sandier layer, but shows the same components of sand mixed with organic-rich pellets of silty clay.

Both samples show that the fine pellety, silty clay fraction material between grains is composed of very thin organo-mineral excrements of mesofauna that represent biological working of guano inputs contemporary with sand blowing and bird/bat activity. Furthermore, the sand/fine silty clay pellet mix demonstrates that sand – whether of marine or aeolian origin – was repeatedly stabilized and exposed subaerially to allow for the accumulation and reworking of organic material by soil mesofauna. No evidence for marine-derived sands could be seen.

Base of main sequence (cave entrance deposits)

A sample of reddish clay sand was collected from a ledge on the north side of the cave entrance at ~1.5 to 2.0 m above sea level.

It is massive and concreted, and forms a ledge (Fig. 4.17); laterally, it grades into sandy deposits mixed with stones and shells. In thin section, it consists of quartzitic sand in a somewhat clayey calcareous matrix (Fig. 4.18). It is a mud-supported rock with clotted texture as in sample Gor98-160. Also present are traces of shells and numerous 30–50 μm dark brown specks and spots, which are probably manganese impregnations. The sample shows calcareous mud associated with aeolian sand which was later cemented by seeping water resulting in the formation of a breccia-like deposit. The pellets show again, as in samples Gor89-01 through Gor89-03, that subaerial reworking by soil mesofauna took place on an exposed surface. The amount of fine fraction, furthermore, suggests that the deposition was likely colluvial as this is a mud-supported deposit. Unfortunately, the cementation has obscured some of the original character of the fine fraction pellets (Fig. 4.18).

The lowermost micromorphological samples (Gor98-160 through Gor98-163) come from this unit. All samples in this section are quite similar. Sample Gor98-160 at the top of the profile comprises medium, well sorted quartzitic sand with bioclasts, micritic clots and coatings, and remnants of possible aeolianite. Bone is present but poorly preserved, and some is associated

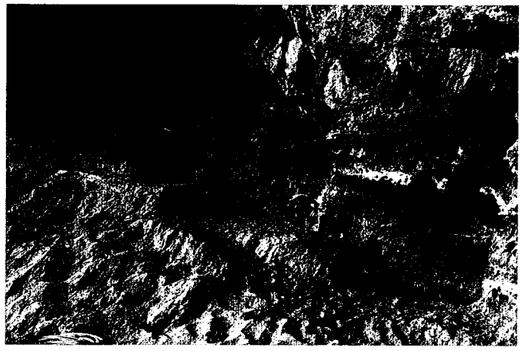

Fig. 4.17 Gorham's Cave, left hand side of cave entrance. A sample of reddish clay sand was collected from this ledge on the north side of the cave entrance at ~1.5 to 2.0 m above sea level; soil micromorphology suggests it was formed by calcareous mud cementation associated with aeolian sand; later cementation by seeping water resulting in the formation of a breccia-like deposit (see Fig. 4.18). Photo: P. Goldberg and R. Macphail.

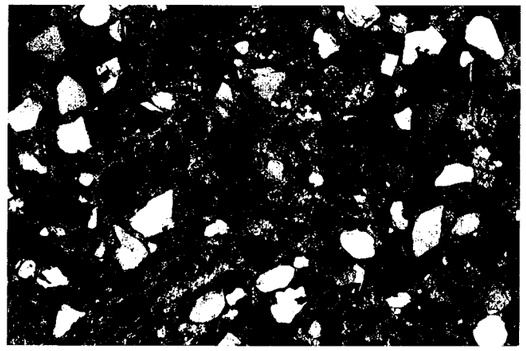

Fig. 4.18 Micromorphology thin-section sample Gor89/32; the sediment is composed of clotted micrite and quartz sand that was later cemented by microsparite. The rounded micro aggregates are mesofaunal excrements and show the presence of reworking of organic material of this subaerial deposit; microsparitic cement resulted from later water saturation. XPL, frame width is ~3.9 mm. Photo: P. Goldberg and R. Macphail.

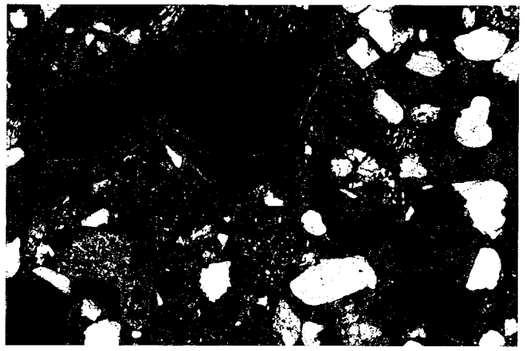

Fig. 4.19 Micromorphology thin-section sample Gor98/162; sandy sediment containing angular piece of algal tufa detached from the walls or cave roof. Its freshness indicates lack of transport and likelihood that the roof extended over this location at the time of deposition during the last Interglacial. Coatings of micrite and with locally clotted appearance. XPL, frame width is ~3.9 mm. Photo: P. Goldberg and R. Macphail.

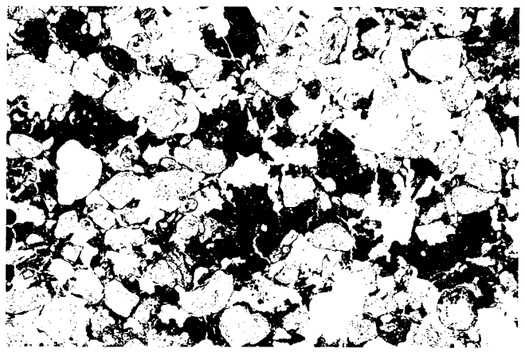

Fig. 4.20 Micromorphology thin-section sample Gor98/164; phosphate and organic-rich guano mixed with quartzitic sand grains; elsewhere clay coatings are present. Clearly this deposit must have formed within the cave (although now exposed by cave mouth retreat). PPL, frame width is ~3.9 mm. Photo: P. Goldberg and R. Macphail.

with calcareous clay. In any case, the sample suggests the possibility of the remains of cave occupation being mixed with locally reworked beach sand. A similar view is seen in sample Gor98-162, which is below Gor98-160. It exhibits more micritic cementation and a greater degree of grain coating, locally with a clotted appearance. Moreover, this sample has a number of pieces of tufa fallen from the roof (Fig. 4.19). Their occurrence strongly suggests that this part of the cave was covered with a roof at the time of accumulation of this sediment. It is not likely that these calcareous fragments were transported very far as they are quite angular, as are the trace amounts of angular bone fragments.

Discussion and conclusions

Sediments, penecontemporaneous and post-depositional processes

A Sand and silt

The major component of the sediments in Gorham's Cave is sand (see Figs. 4.2, 4.3, 4.7 and 4.8). This is derived either from direct aeolian inputs or from continual reworking of sand, ultimately of aeolian origin, but derived either locally from adjacent deposits or from outside the cave. As there have been a number of slumping events, local reworking is a reasonable assumption. Also, because of the slumping and predominant 'depositional dip' inwards originating from the possible presence of a dune in front of the cave, as clearly demonstrated by the sequence at Vanguard Cave (see Chapter 13), some of the sediment could be derived from closer to the entrance, either as aeolian grain fall or as colluvium. Certainly, there is evidence for inwashing of silt and clay clearly derived from soils overlying the cave, as shown by the soil aspect of the material in thin section (cf. Vanguard Cave, Figs. 13.16 and 13.17), numerous graded beds, and the fact that both textural classes are not produced within the cave confines. Thus, some reworking of sand with this wash is likely although volumetrically this is not a major factor in importing sand into the cave (e.g. samples Gor96-56, Gor96-59).

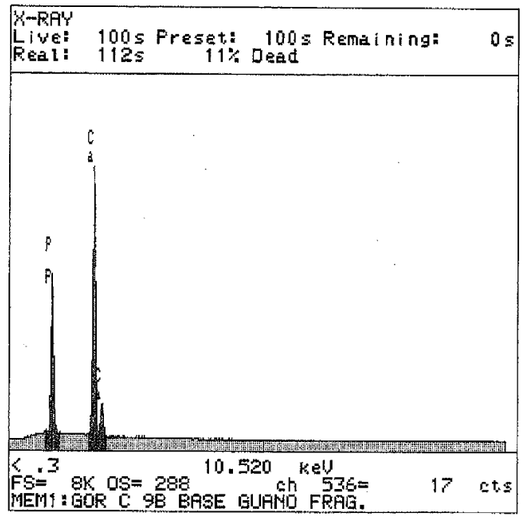

Fig. 4.21 EDAX analysis of Gor89/9B showing peaks of P and Ca identifying calcium phosphate (here guano).

B. Phosphate

Almost all sediments show the direct or indirect effects of inputs of guano, *sensu lato* (see Appendix 4.1; Fig. 4.21; see also Figs. 4.7–4.9 and 4.11–4.14). Such inputs are demonstrated by several micromorphological features, which include 1) phosphatic crusts that accreted during periods of local stabilization when bird and bat guano could accumulate on the surface (see samples Gor89-8, Gor89-10, Gor95-47, Gor98-164 and Gor98-165). Such crusts appear throughout the entire sequence at Gorham's Cave (see also Fig. 13.21). 2) Ubiquitous flecked or pellety microfabrics (e.g. samples Gor89-8, Gor89-5, Gor89-19, Gor95-47, Gor96-55, Gor97-65), which are microfaunal excrements that represent insect reworking of organic inputs by bird/bat droppings. For Gorham's Cave it is reasonable to imagine a rich surface fauna reworking guano accumulations. (The chief factor cited to explain the lack of preserved pollen in these sediments is biological working and oxidation; Gill Cruise, pers. comm.). Cave guano insect fauna are also well known, as discussed in Gillieson (1996, 233). Other phosphate inputs are carnivore coprolites, particularly hyaena (see Chapter 19). Hyaena activity and individual whole coprolite remains are particularly visible in the upper deposits (e.g. samples Gor89-28 – elevation of 1445, UBSm, Gor96-51, Gor89-23), where in the initial season of 1989 a dark organic layer exhibited a stringer of several individual, whole coprolites of hyaenas. Many thin sections from this layer and above contain coprolite fragments (Figs. 4.22 and 4.23; see Chapter 19), generally including whole ones, as clearly visible in the field. Finally, phosphate alteration derived from guano is expressed by fallen pieces of roof (e.g. macroscan of Gor89-28b), in which limestone bedrock develops weathering rinds of apatite (probably dahllite). These rinds commonly break off as thin 'exfoliation' crusts and become incorporated into the deposits. Again, sediments from the upper part of the profile are relatively rich in this material.

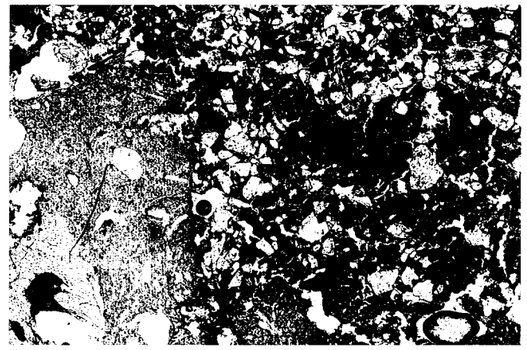

Fig. 4.22 Micromorphology thin-section sample Gor98/155; a piece of hyaena coprolite with grey calcined bone fragment (see Chapter 18). PPL, frame width is ~3.9 mm. Photo: P. Goldberg and R. Macphail.

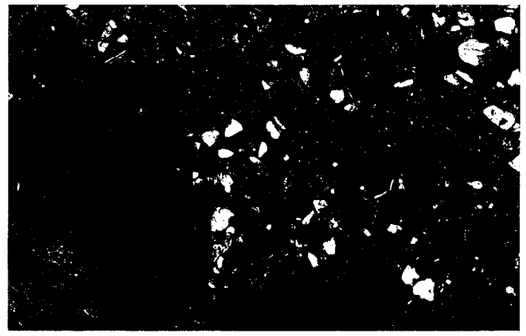

Fig. 4.23 Micromorphology thin-section sample Gor98-155, as above but in XPL; note typical isotropic nature of coprolite (apatite). Photo: P. Goldberg and R. Macphail.

C. Calcite

Cementation by calcite is patchy throughout the section. It is striking in the lower units, where cementation occurs as lenses that thicken in the direction of the large pillar on the north side of the cave (Square B110). It is also evident in upper deposits CHm and UBSm. Furthermore, it is possible that calcite cementation was more widespread, but since many of the deposits are non-calcified (particularly in the central section) or have been decalcified, it is difficult to evaluate clearly the effects of calcite cementation, let alone its hydrological and climatic significance. The acid nature of guano and organic matter accumulation is adverse to calcite preservation.

In certain cases, two phases of calcite precipitation are evident: first a micritic, clotted-micrite phase in which grains become coated; this is followed by a second phase, which is characterized by the precipitation of microsparite within intergranular voids (see Figs. 4.15, 4.16 and 4.18). These two successive phases would seem to point to a change in regime from calcite precipitation first under evaporative conditions thus coating the grains, followed by less evaporative and more water-saturated conditions producing the microsparite. As such, it may be indicative of conditions occurring more on a regional scale, such as climatic conditions of greater overall precipitation.

D. Human activity

Human inputs are variously striking or subtle (see Figs. 4.4–4.6, 4.11 and 4.12). Striking inputs take the form of charcoal-rich horizons that can be readily seen in the field as combustion features, as at the top of the stratigraphic profile in the Upper Palaeolithic deposits (sample Gor97-68), but also in the sandier areas of the Middle Palaeolithic sediments, where sandy deposits are enriched in charcoal. For the most part, the latter, charcoal-rich sands do not represent *in situ* burning features but rather scatters of charcoal that have been displaced from their original location of combustion, even if only on the scale of centimetres. Charcoal was mobilized by wind and also by trampling, as can be seen in the rather chaotic organization of this material (e.g. Gor96-52, Gor95-47, Gor96-57) (Fig. 4.24; see Figs. 4.4 and 4.5). Intact combustion features, such as those at Kebara Cave, are rare to non-existent at Gorham's Cave, except possibly for those features at the top of the section

Also interesting at Gorham's Cave is the general lack of carbonate ashes, although cemented ashes can be found in the Upper Palaeolithic deposits. This is intriguing in light of the amount of burnt bone and charcoal observed in many of the thin sections. The lack of ashes might be related to the fact that they got blown away as the site is quite exposed; ashes are quite light and fluffy and would not be expected to remain, or they would become cemented quickly (Karkanas and Goldberg 2008). Alternatively, there was incomplete combustion and the charcoal was not reduced completely to ashes, although this seems a rather remote possibility as many bones are burnt; and if wind is a factor, then most fires should have been hot enough to sustain complete combustion, unless they were terminated early. Finally, ashes were originally present but were dissolved, or diagenetically altered by phosphate mineralization. Decalcification is an ongoing process at Gorham's and most deposits show the effects of carbonate dissolution; calcite does not appear to be precipitating in any of the deposits today from dripping water. Phosphate mineralization was observed at Kebara Cave, where ashes can be transformed into apatite. Although the original ash rhombs are not visible in normal transmitted light illumination, they can be seen using ultra violet and blue light illumination. Unfortunately, we did not make extensive observations in blue light of all the Gorham's thin sections but in those that were studied in 1989 we could plainly see the guano particles, suggesting an agent for decalcification (see sample Gor85-14 (Figs. 4.13 and 4.14), and Vanguard Cave (Figs. 13.4 and 13.21–13.28).

Subtle human inputs are represented by thin charcoal stringers or accumulations that are not differentiable as intact features in the field. In the case of sample Gor95-47, for example, the charcoal is finely laminated, and was deposited by sheet flow or washed into very shallow pools of water. In fact, the LBSm is characterized by features indicative of water deposition. Even in the lower deposits in the cave observed by us (samples Gor89-160 through Gor89-163), isolated sand-size scraps of charcoal were observed.

There is a marked coincidence between the presence of burned debris and enhanced magnetic susceptibility (Appendix 4.1), which reinforces the view that Middle

Fig. 4.24 Micromorphology thin-section sample Gor96-52; macroscan showing a complex sample composed of silty/clayey sand at the base, a band of charcoal and burned bone in the centre, and a capping of more uniform quartz sand. The chaotic nature of the burned materials suggests trampling or hearth rake-out (see Figs. 4.4 and 4.5). Frame height is ~50 mm. Photo: P. Goldberg and R. Macphail.

Palaeolithic hearths were present (see relationship between well preserved combustion zones in Vanguard Cave, Figs. 13.11, 13.31 and 13.32) but have been reworked downslope and are no longer visible in their original locations.

Conclusions

In short, both field observations by us between 1989–1998 and micromorphological results show that much of the geological history of the cave is represented by sand inputs penecontemporaneous with those of organic silty clay washed in from outside or derived from joints in the cave (as at Vanguard, Chapter 13), coupled with bird/bat guano, and punctuated by human occupation and that of hyaenas. Depending on the relative rates of occupation of these sources, we observe either massive sands, or sands with stringers of guano (e.g. samples Gor98-16, Gor98-165; Figs. 4.10–4.12) that represent short standstill periods of sand accumulation. All these findings are corroborated by the bulk data.

The cave at the time of the earliest deposition was probably more closed and the brow/entrance extended further out than it does today. This statement is supported by, and consistent with, the presence of pellety, guano-related microfabrics that indicated a semi-enclosed environment; fragments of carbonate ornaments ('algal/biological' crusts) formed on the cave ceiling and walls; and the presence of clay coatings (though weak) in sample Gor98-164. These coatings indicate subaerial and somewhat protected exposure, which is possibly related to dripping water.

The earliest occupation of the cave could have taken place during the formation of the lowermost sediments exposed at the cave entrance, in which there are fragments of bone and some traces of charcoal. The presence of these materials does not necessarily indicate that these are the remains of human occupation, but the evidence is quite suggestive. In fact, it is necessary to consider that they represent colluvial reworking of cultural deposits that are no longer visible, as is the case in Vanguard with the absence of the Middle Palaeolithic hearths/combustions (Macphail and Goldberg

2000; Chapter 13). Logically, this could also be a reflection of how the sedimentary sequence at Gorham's Cave is more complicated than at Vanguard Cave, where rapid sedimentation with only very localized reworking of hearths seems to have taken place.

Acknowledgements

The authors thank the National Geographic Society for funding this research, and the Natural History Museum and Gibraltar Museum for discussion, collaboration and support, and especially through Chris Stringer and Clive Finlayson, respectively. Like all the contributors we are very grateful to Nick Barton (Oxford University) for overall discussion, and for organizing, integrating and editing this volume. We also thank Simon Collcutt and Andy Currant for providing the lithostratigraphic framework for this chapter. The Institute of Archaeology, University College London is also thanked for support especially through Sandra Bond (SEM/EDXRA), Kevin Reeves (microprobe) and Cyril Bloomfield (analysis of Phosphorus); additional analyses including magnetic susceptibility were carried out by Johan Linderholm (Environmental Archaeology Laboratory, Umeå University, Sweden), who is gratefully acknowledged. Thin sections were manufactured at the Natural History Museum, and by Spectrum Petrographics (Vancouver, Washington, USA). In addition we gratefully thank the following for all their various contributions to this study: Peter Andrews, Nick Barton, Gerry Black, Andy Currant, Clive and Geraldine Finlayson, Lorraine Cornish, Jo Cooper, Yolanda Fernández-Jalvo, Frank Greenway and Chris Stringer.

References

Gillieson, D. 1996: Caves: *Processes, Development, Management* (Oxford: Blackwell).

Goldberg, P. and Macphail, R.I. 2000: Micromorphology of Sediments from Gibraltar Caves: Some Preliminary Results from Gorham's Cave and Vanguard Cave. In Finlayson, C., Finlayson, G. and Fa, D. (eds.), *Gibraltar During the Quaternary* (Gibraltar: Gibraltar Government Heritage Publications, Monograph 1), 93–108.

Karkanas, P. and Goldberg, P. 2008: Micromorphology of sediments: Deciphering archaeological context. *Israel Journal Earth Sciences* 56, 63–71.

Macphail, R.I. and Goldberg, P. 2000: Geoarchaeological investigation of sediments from Gorham's and Vanguard Caves, Gibraltar: Microstratigraphical (soil micromorphological and chemical) signatures. In Stringer, C.B., Barton, R.N.E. and Finlayson, J.C. (eds.), *Neanderthals on the Edge* (Oxford: Oxbow Books), 183–200.

Shahack-Gross, R., Berna, F., Karkanas, P. and Weiner, S. 2004: Bat guano and preservation of archaeological remains in cave sites. *J. Archaeol. Sci.* 31, 1259–1272.

Wattez, J., Courty, M.A. and Macphail, R.I. 1990: Burnt organomineral deposits related to animal and human activities in prehistoric caves. In Douglas, L.A. (ed.), *Soil Micromorphology: a basic and applied science* (Amsterdam: Elsevier), 431–441.